

# Heterogeneous Gold Catalyst: Synthesis, Characterization, and Application in 1,4-Addition of Boronic Acids to Enones

Alaina Moragues,<sup>†</sup> Florentina Neațu,<sup>\*,‡,§</sup> Vasile I. Pârvulescu,<sup>\*,‡</sup> Maria Dolores Marcos,<sup>||</sup> Pedro Amorós,<sup>\*,†</sup> and Véronique Michelet<sup>\*,⊥</sup>

<sup>†</sup>Instituto de Ciencia de los Materiales, Universitat de València, P.O. Box 22085, 46071 Valencia, Spain

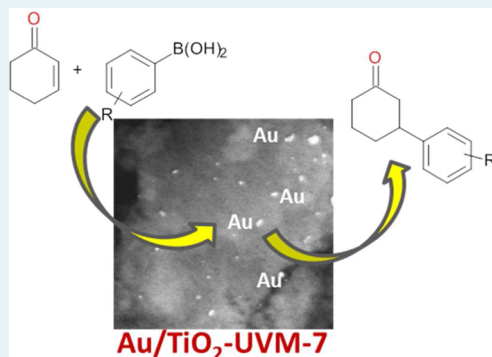
<sup>‡</sup>Department of Organic Chemistry, Biochemistry and Catalysis, University of Bucharest, 4-12 Regina Elisabeta Boulevard, 030016 Bucharest, Romania

<sup>§</sup>National Institute of Materials Physics, Laboratory of Optical Processes in Nanostructured Materials, 105Bis Atomistilor Street, P.O. Box MG7 Magurele, Bucharest, Romania

<sup>||</sup>Centro de Reconocimiento Molecular y Desarrollo Tecnológico (IDM), Departamento de Química, Universidad Politécnica de Valencia, Camino de Vera s/n, 46022 Valencia, Spain

<sup>⊥</sup>PSL Research University, Chimie ParisTech-CNRS, Institut de Recherche de Chimie Paris, 11 rue P. et M. Curie, 75005 Paris, France

**ABSTRACT:** The new 1 wt % Au/TiO<sub>2</sub>–UVM-7 catalyst was prepared and fully characterized. This heterogeneous catalyst proved to be active, selective and recyclable for the unprecedented gold-catalyzed 1,4-addition of various functionalized arylboronic acids to 2-cyclohexen-1-one and other selected enones using toluene as a solvent. The gold-based catalyst was recycled two times and played an active role in this reaction, and the nature of the solvent determined a remarkable change in the products' selectivities.



**KEYWORDS:** heterogeneous catalysis, gold, 1,4-addition, boronic acids, selectivity, solvent effect

## 1. INTRODUCTION

Nano and subnano gold particles have shown very interesting applications in catalysis with very high selectivities and TONs in multiple reactions.<sup>1</sup> Most of these examples refer to supported gold nanoparticles, in which the support has either the role of stabilizing gold species in different oxidation states (Au<sup>δ+</sup>, Au<sup>+</sup>, or Au<sup>3+</sup>)<sup>1a,2</sup> or the role of ensuring a buffer electron transfer to these nanoparticles. This interaction differentiates among the reactions in which these catalysts have been investigated.<sup>3</sup> Among these, gold nanoparticles were reported to exhibit activity in carbon–carbon (C–C) coupling reactions. Conventionally, gold-catalyzed C–C bond formations were merely investigated using homogeneous catalytic systems, which exhibit very high TONs but suffer from the isolation/recycling point of view.<sup>4</sup> Heterogeneous gold-supported catalysts were, however, reported in these reactions as well: homocoupling reactions,<sup>5</sup> cross-coupling,<sup>6</sup> Suzuki–Miyaura cross-coupling,<sup>7</sup> Sonogashira cross-coupling,<sup>8</sup> Ullmann coupling,<sup>9</sup> sequential oxidation addition reactions,<sup>10</sup> benzylation of aromatics,<sup>11</sup> oxidative C–C coupling reactions,<sup>12</sup> amination reactions,<sup>13</sup> cycloisomerization reactions,<sup>14</sup> and nucleophilic addition.<sup>15</sup>

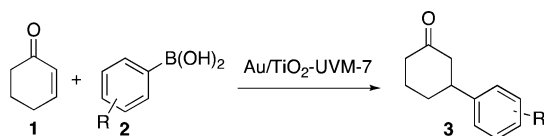
1,4-Addition of arylboronic acids to  $\alpha,\beta$ -unsaturated ketones is another C–C bond coupling of broad interest.<sup>16</sup> Few reports about the addition of arylboronic acids to 2-cyclohexenone in the presence of heterogeneous catalysts have been described so far in the literature,<sup>17</sup> and all of them refer to rhodium complexes. We have selected UVM-7, a nanoparticulated material with a bimodal pore system,<sup>18</sup> as the heterogeneous support. The most outstanding feature concerning this nanostructured material is its peculiar (very open) architecture, which is based on a continuous network constructed from covalently bonded mesoporous nanoparticles, whose aggregation defines a non-ordered secondary system of large pores. The intraparticle mesopore micelle template system has similarities to the one present in MCM-41-like solids<sup>19</sup> and could therefore be modified to include TiO<sub>2</sub> domains on the silica surface and later gold nanoparticles. The existence of hierarchic porosity, combined with short-length mesopores, favors impregnation and subsequent TiO<sub>2</sub> dispersion in a highly homogeneous way. These TiO<sub>2</sub> nanodomains are able to act as

Received: June 9, 2015

Revised: July 16, 2015

preferred inorganic anchors for the gold nanoparticles and, due to the open framework of UVM-7, will present an enhanced accessibility. Having these specific characteristics in mind, we therefore embarked on the synthesis of a Au/TiO<sub>2</sub>–UVM-7 catalyst, anticipating superior activity compared with other gold heterogeneous systems. As part of our ongoing program toward applications of supported gold nanoparticles in catalysis,<sup>14d,20</sup> we wish therefore to report herein our preliminary results on the preparation of gold supported on mesoporous UVM-7 silica and its unprecedented use in 1,4-addition of various arylboronic acid (2) to 2-cyclohexen-1-one (1) (Scheme 1) and other selected enones.

**Scheme 1.** 1,4-Addition of Arylboronic Acids to 2-Cyclohexen-1-one



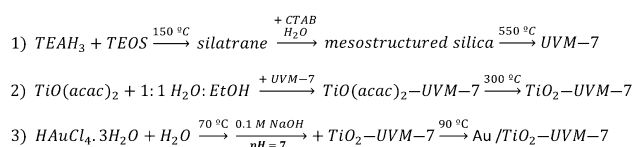
## 2. EXPERIMENTAL PART

**2.1. Catalysts Preparation.** The synthesis of UVM-7 is based on the atrane route, a general preparative strategy previously described in detail.<sup>18</sup> Once the UVM-7 mesostructured solid was obtained, to prepare the final porous material, the template was removed by calcination at 550 °C for 6 h (heating ramp = 5 °C·min<sup>-1</sup>) under static air atmosphere.

Once the silica support was prepared, it was loaded with 3.7 wt % of Ti/(Ti + SiO<sub>2</sub>) in a way similar to that described elsewhere.<sup>20</sup> The corresponding amount of titanylacetylacetonate (TiO(acac)<sub>2</sub>) (0.19 g) was mixed with 100 mL of ethanol and vigorously stirred. Subsequently, deionized water (100 mL) was slowly added. After that, the UVM-7 silica support (0.6 g) was stirred for 2 h with the Ti solution. The mixture was filtered, washed, and allowed to dry overnight at room temperature. The TiO<sub>2</sub>–UVM-7 was calcined at 300 °C for 5 h (heating ramp = 1 °C·min<sup>-1</sup>) under static air atmosphere. This silica–titania support was then loaded with 1 wt % of Au/(Au + support) (nominal composition) by a deposition–precipitation method. Working in a 70 °C oil bath, 10 mg of HAuCl<sub>4</sub>·3H<sub>2</sub>O was added to 50 mL of water, and the pH was adjusted to 7 using 0.1 M NaOH. The impregnation on 0.5 g of TiO<sub>2</sub>–UVM-7 was then carried out for an hour. The mixture was filtered, washed, and dried at 90 °C overnight (Au/TiO<sub>2</sub>–UVM-7, Scheme 2). The heterogeneous catalysts 1 wt % Au/SiO<sub>2</sub>, 1 wt % Au/UVM-7, and 1 wt % Au/TiO<sub>2</sub> were prepared by the same deposition–precipitation method as used for the Au/TiO<sub>2</sub>–UVM-7 catalyst.

**2.2. Catalyst Characterizations.** The chemical analysis of the materials was performed using an XL 30 ESEM instrument

**Scheme 2.** Three-Step Preparation Procedure of Au/TiO<sub>2</sub>–UVM-7 Catalyst



equipped with EPMA (electron probe microanalysis). Powder X-ray diffraction patterns were recorded with a Seifert 3000TT  $\theta$ – $\theta$  diffractometer using Cu K $\alpha$  radiation. The TEM and HRTEM microstructural characterizations were carried out using a JEOL JEM-1010 instrument operating at 100 kV and equipped with a CCD camera and a Tecnai G<sup>2</sup>F20(FI) instrument, respectively. STEM–HAADF (scanning transmission electron microscopy–high-angle annular dark-field) images were acquired on a JEOL-2100F microscope. The N<sub>2</sub> adsorption–desorption isotherms were recorded at –196 °C using a Micromeritics ASAP2020 automated instrument. Calcined samples were degassed for 15 h at 130 °C and 10<sup>–6</sup> Torr before analysis. Surface areas were estimated according to the BET model, and pore size dimensions were calculated using the BJH method. Raman spectroscopy was performed using a Horiba spectrometer equipped with a He–Ne ( $\lambda$  = 633 nm) laser. The spectra were recorded in the 200–4000 cm<sup>–1</sup> range.

**2.3. Catalytic Tests.** To a mixture of arylboronic acid (2.30 mmol), Na<sub>2</sub>CO<sub>3</sub> (0.92 mmol), 2-cyclohexen-1-one (0.46 mmol), and toluene (4 mL) was added 30 mg of catalyst. The reaction mixture was heated at 80 °C until completion of the reaction (TLC) and then cooled to room temperature. The reaction mixture was filtered on a short pad of silica gel with cyclohexane/ethyl acetate (7:3) and evaporated under reduced pressure. No further purification was necessary. The purity of the product (>98%) was checked by <sup>1</sup>H and <sup>13</sup>C NMR and GC/MS analyses.<sup>15,16</sup> To investigate the chemical stability of the catalysts, the content of the leached metal into the reaction liquid was determined by ICP–OES (Agilent Technologies, 700 series).

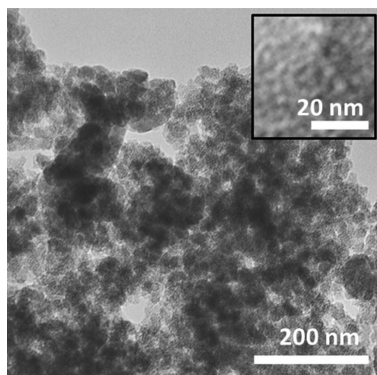
## 3. RESULTS AND DISCUSSIONS

**3.1. Catalyst Characterizations.** The UVM-7 silica is a mesoporous material with a hierarchic porosity, with large interparticle voids and 3D interconnected mesopores. This open framework endows the material with enhanced accessibility, favoring mass diffusion throughout the hierarchical pore structure.<sup>18c</sup> These structural features are highly beneficial for the next stage of synthesis, the addition of Ti. The open nature of the support favors a regular and homogeneous impregnation with the titanium complex solution. Then the material is loaded with TiO<sub>2</sub> using a simple wet impregnation of UVM-7 with titanium(IV) oxyacetylacetonate and calcining the samples at 300 °C.<sup>21</sup>

We have used EPMA to verify the chemical homogeneity of the resulting TiO<sub>2</sub>–UVM-7 solids. Table 1 gathers the data corresponding to the bulk chemical composition. These values have been calculated by averaging EPMA data of ~20 different particles. The relatively low standard deviation of the measurements allows us to reasonably assume that the TiO<sub>2</sub>–UVM-7 sample is chemically homogeneous with a regular dispersion of Ti species on the silica walls. The incorporation of TiO<sub>2</sub> domains does not alter the UVM-7 organization. The TEM image in Figure 1 shows that the bimodal nanoparticle topology, typical of UVM-7 solids, is preserved. Both intra- and interparticle pores can be clearly distinguished. The N<sub>2</sub> adsorption–desorption isotherm (Figure 2) is in good accordance with TEM image. The relatively low proportion of TiO<sub>2</sub> domains included in the UVM-7 mesostructure allows preserving high values of the surface area and pore volume (similar to typical values observed for pure UVM-7 silica).

Table 1. Selected Preparative and Physical Data

sample	nominal content M/M <sup>+</sup> support (% wt)		EPMA results M/M + support (% wt)		BET area (m <sup>2</sup> /g)	BJH volume (cm <sup>3</sup> /g)
	M = Ti	M = Au	M = Ti	M = Au		
TiO <sub>2</sub> -UVM-7	3.7		3.8 ± 0.3		1028.7	1.74
Au/TiO <sub>2</sub> -UVM-7	3.8	1.0	4.6 ± 0.7	1.6 ± 0.3	697.7	1.56

Figure 1. TEM image of the TiO<sub>2</sub>-UVM-7 sample.

As expected, the soft experimental conditions used during the Au deposition (neutral pH and 70 °C) ensure the conservation of the UVM-7-type organization to a great extent. The two adsorption steps and their respective peaks in the BJH pore size distribution can be observed for the gold-containing material (Figure 2). However, although the gold incorporation implies an appreciable decrease in both the BET area and the BJH pore volume, the final catalyst yet preserves a high and accessible porosity. The preservation of the UVM-7 meso-structure is further supported by TEM images in Figure 3. We observe the typical aggregates of mesoporous nanoparticles describing the bimodal pore organization. The HAADF micrographs display a good gold dispersion. The HRTEM shows the existence of ordered nanodomains associated with the gold and the TiO<sub>2</sub> particles included on the amorphous silica surface.

The small size of these ordered domains prevents their detection by XRD techniques. In fact, the XRD powder pattern of the Au/TiO<sub>2</sub>-UVM-7 sample shows only large signals

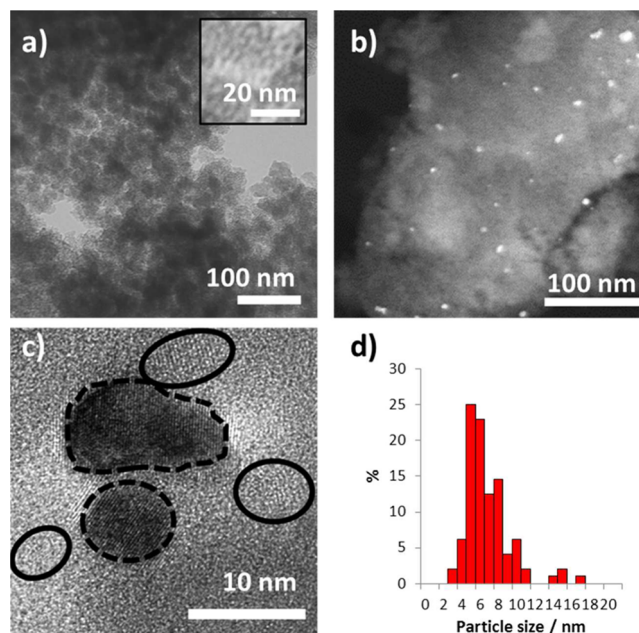


Figure 3. (a) TEM, (b) HAADF, and (c) HRTEM images of the Au/TiO<sub>2</sub>-UVM-7 sample (domains highlighted with dashed and continuous lines correspond to gold and anatase particles, respectively) and (d) gold particle size distribution histogram.

associated with the amorphous silica support. There are no peaks that can be attributed to crystalline gold or TiO<sub>2</sub>. Titania is found as anatase with a small part of rutile. As can be seen in the Raman spectra in Figure 4, the sample presents the three characteristic peaks of anatase with shoulders that can be associated with the rutile structure.

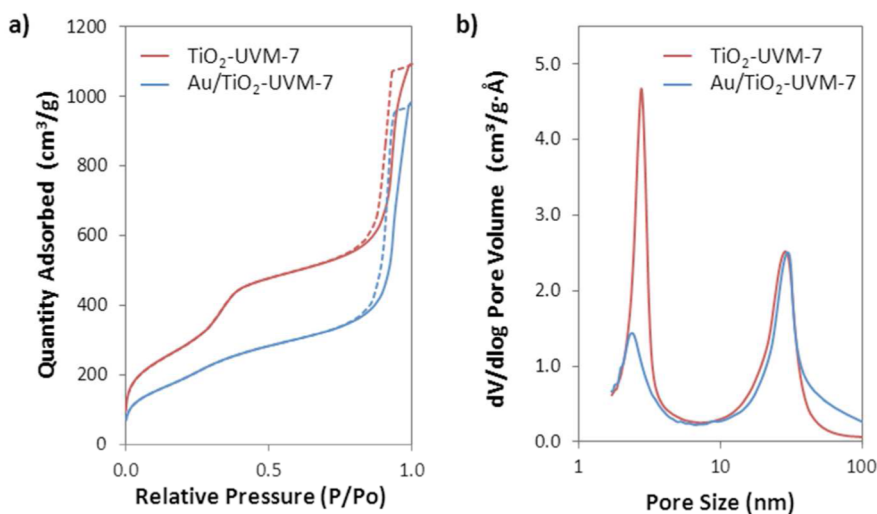
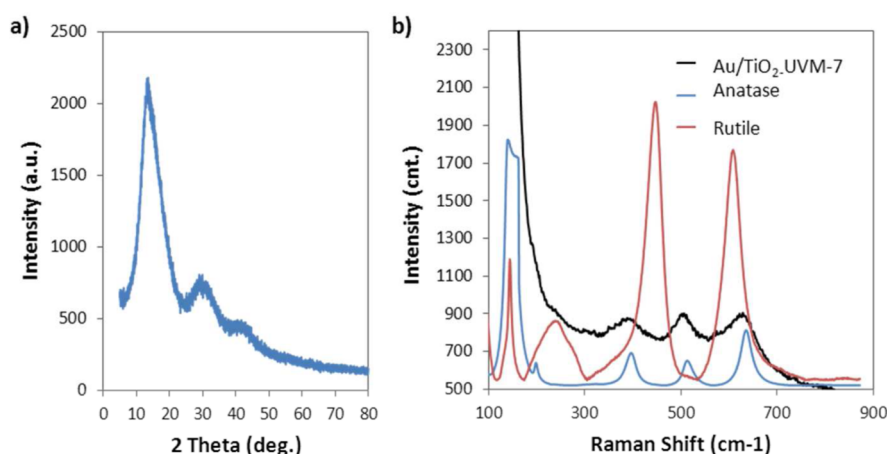
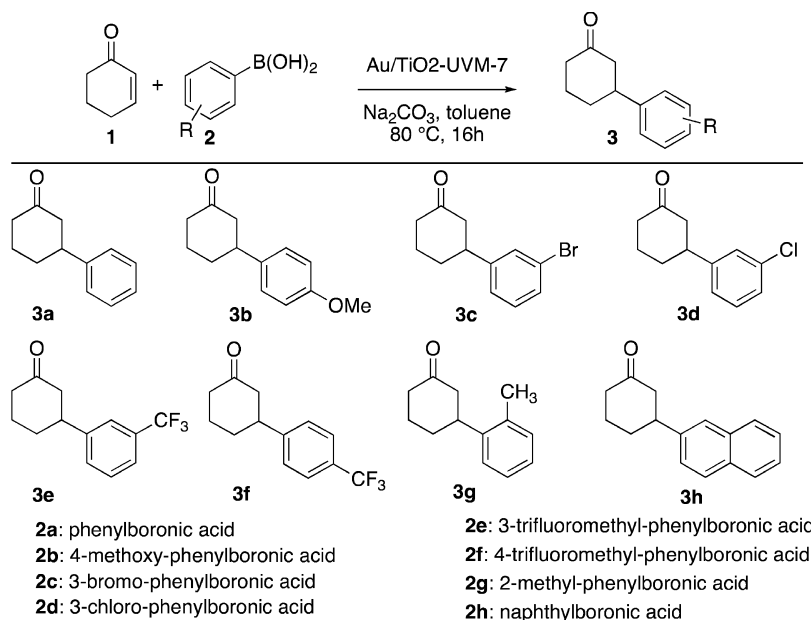


Figure 2. (a) N<sub>2</sub> adsorption-desorption isotherms and (b) BJH pore size distributions of TiO<sub>2</sub>-UVM-7 and Au/TiO<sub>2</sub>-UVM-7 samples.



**Figure 4.** (a) High-angle XRD pattern and (b) Raman spectrum of Au/TiO<sub>2</sub>-UVM-7 sample. The Raman spectra of anatase and rutile have been included for comparison.

**Table 2.** 1,4- Addition of Arylboronic Acid (**2**) to 2-Cyclohexen-1-one (**1**) over Au/TiO<sub>2</sub>-UVM-7 Heterogeneous Catalyst<sup>a</sup>



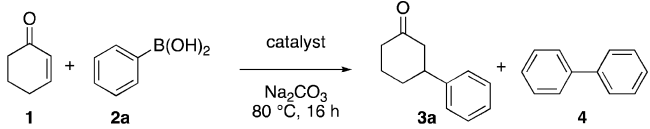
entry	R-C <sub>6</sub> H <sub>4</sub> -B(OH) <sub>2</sub>	product	conversion <sup>b</sup> (%)	yield <sup>c</sup> (%)
1	<b>2a</b> R: -H	<b>3a</b>	98	95
2	<b>2b</b> R: -OCH <sub>3</sub> (para)	<b>3b</b>	55	53
3	<b>2c</b> R: -Br (meta)	<b>3c</b>	66	64
4	<b>2d</b> R: -Cl (meta)	<b>3d</b>	64	61
5	<b>2e</b> R: -CF <sub>3</sub> (meta)	<b>3e</b>	87	85
6	<b>2f</b> R: -CF <sub>3</sub> (para)	<b>3f</b>	88	86
7	<b>2g</b> R: -CH <sub>3</sub> (ortho)	<b>3g</b>	60	57
8	<b>2h</b> naphthylboronic acid	<b>3h</b>	0	0

<sup>a</sup>1 equiv of **1** (0.46 mmol), 5 equiv of **2**, 2 equiv of Na<sub>2</sub>CO<sub>3</sub>, toluene (4 mL), 30 mg of catalyst 1% Au/TiO<sub>2</sub>-UVM-7, 80 °C, 16 h. <sup>b</sup>Determined by GC. <sup>c</sup>Isolated yield.

**3.2. Catalytic Tests.** Having prepared and characterized the Au/TiO<sub>2</sub>-UVM-7 catalyst, we decided to investigate its use in an original and novel process implying boronic acids. Indeed, inspired by the seminal work of Corma on heterogeneous gold-catalyzed homocoupling of boronic acids,<sup>5d-f</sup> we wondered if arylgold species could add to 2-cyclohexen-1-one. Table 2 compiles results evidencing the role of the substituent of the boronic acid in the 1,4-addition of **2** to **1** using the Au/TiO<sub>2</sub>-UVM-7 catalyst.

Pleasingly, we observed the desired formation of the arylated ketone when reacting enone **1** with phenylboronic acid in the presence of gold catalyst. Depending on the aromatic ring of the boron derivative, the yields varied from 0% (for naphthylboronic acid) to 95% for the nonsubstituted one (Table 2, entries 1–8). It is worth noting that the addition of phenylboronic acid to 2-cyclohexen-1-one in the presence of only 0.33 mol % of gold (Table 2, entry 1) occurred with a TOF (turn over frequency) of 18 (in 16 h), that is, 3–4 times



Table 3. Catalyst and Solvent Influences in the 1,4-Addition of Phenylboronic Acid (2a) to 2-Cyclohexen-1-one (1)<sup>a</sup>


entry	catalyst	solvent	conversion <sup>b</sup> (%)	3a yield <sup>c</sup> (%)	4 yield <sup>c</sup> (%)
1	Au/TiO <sub>2</sub> –UVM-7	toluene	98	95	
2	Au/SiO <sub>2</sub>	toluene	11	n.d.	
3	Au/UVM-7	toluene	23	n.d.	
4	Au/TiO <sub>2</sub>	toluene	70	n.d.	
5	TiO <sub>2</sub> –UVM-7	toluene			
6		toluene			
7	Au/TiO <sub>2</sub> –UVM-7	toluene/water <sup>d</sup>	94	90	1
8	Au/TiO <sub>2</sub> –UVM-7	toluene/water <sup>e</sup>	95	61	30
9	Au/TiO <sub>2</sub> –UVM-7	water	80	34	44
10	Au/TiO <sub>2</sub> –UVM-7	methanol	82	36	43

<sup>a</sup>1 equiv of 1 (0.46 mmol), 5 equiv of 2, 2 equiv of Na<sub>2</sub>CO<sub>3</sub>, solvent (4 mL), 30 mg of catalyst. <sup>b</sup>Determined by GC. <sup>c</sup>Isolated yield reported to 2-cyclohexen-1-one. <sup>d</sup>4.9 mL toluene/0.1 mL water. <sup>e</sup>2 mL toluene/2 mL water.

higher than those reported on other heterogeneous catalytic systems.<sup>17</sup> The use of substituted phenylboronic acids led to lower isolated yields (55–86%) of the corresponding ketones 3b–3g (Table 2, entries 2–7). Both steric and electronic effects could explain this behavior. A lower yield was obtained for hindered boronic acid such as *ortho*-methylphenylboronic acid (Table 2, entry 7). The high steric influence on the reaction was also demonstrated by the nonreactivity of 2-naphthylboronic acid, which is the organometallic partner bearing the bulkiest group (Table 2, entry 8). Moderate reactivity was observed in the case of electron-rich boronic acid, such as the *para*-methoxyphenylboronic acid, most plikely as a result of a slower transmetalation step and, therefore, competitive protodeboronation reaction. Very good yields were observed in the case of boronic acids bearing electron-withdrawing groups, the best results being obtained, as anticipated, for trifluoromethyl substituents, having the strongest electron-withdrawing effects in the series (–Br < –Cl < –CF<sub>3</sub>). The ketones 2e and 2f were isolated in 85% and 86% isolated yields, respectively (Table 2, entries 5–6).

In an effort to validate the role of the support, catalytic tests were performed using Au/TiO<sub>2</sub>, Au/SiO<sub>2</sub>, and Au/UVM-7 catalysts (Table 3). The heterogeneous catalysts Au/SiO<sub>2</sub> and Au/UVM-7 (1 wt %) exhibited a low activity for the 1,4-addition of phenylboronic acid to 2-cyclohexen-1-one (Table 3, entries 2, 3). The small difference between these catalysts is most probably attributable to the open architecture of UVM-7, allowing a better dispersion of gold. The use of 1 wt % Au/TiO<sub>2</sub> allowed the formation of the desired ketone 3a (Table 3, entry 4), but with a lower conversion compared with the use of Au/TiO<sub>2</sub>–UVM-7 complex (Table 3, entry 1). The superior activity of the Au/TiO<sub>2</sub>–UVM-7 catalyst may be explained by the high dispersion of Au combined with a specific interaction of Au with the dispersed titanium oxide and also by the existence of a high accessibility to the active sites, thanks to the hierarchical porosity of UVM-7 combined with the short-length mesopores. Blank experiments carried out in the absence of catalyst (Table 3, entry 6) and in the presence of the support (Table 3, entry 5) did not result in product formation, thus demonstrating the catalytic activity of Au nanoparticles.

Considering previous findings in the presence of rhodium heterogeneous catalysts,<sup>17b</sup> we also envisaged studying the

influence of water in this reaction. Thus, phenylboronic acid was allowed to react in the presence of a catalytic amount of the catalysts, in biphasic reaction media (1:1 vol/vol ratio of toluene and water), in air at 80 °C. Water addition to the reaction media resulted in the appearance of a byproduct (biphenyl) not observed under previous conditions (toluene). Interestingly, the formation of biphenyl is proportional to the amount of water added to the system (Table 3, entries 7–8). This result is in agreement with previous studies on homocoupling of phenylboronic acid over gold nanoparticles,<sup>5d–f</sup> which demonstrate the formation of biphenyl in aqueous media, in contrast with a nonpolar solvent, such as toluene, in which the formation of biphenyl does not occur. Performing the reaction only in water (Table 3, entry 9) afforded a conversion of 80%, with an increased selectivity (56%, 44% isolated yield) toward the biphenyl byproduct. Choosing methanol as solvent gave results similar to those for the reaction performed in water (Table 3, entry 10). Obviously, carrying out the reaction in a polar medium led to a competitive reaction between the 1,4-addition of 2 to 1 versus homogeneous coupling of phenylboronic acid.

It is noteworthy that the heterogeneous catalyst Au/TiO<sub>2</sub>–UVM-7 (Table 4, entry 1) has a similar excellent activity or

Table 4. Comparison between Au/TiO<sub>2</sub>–UVM-7 and Other Rh Heterogeneous Catalytic Systems Able To Promote the 1,4-Addition of Phenylboronic Acid to 2-Cyclohexen-1-one

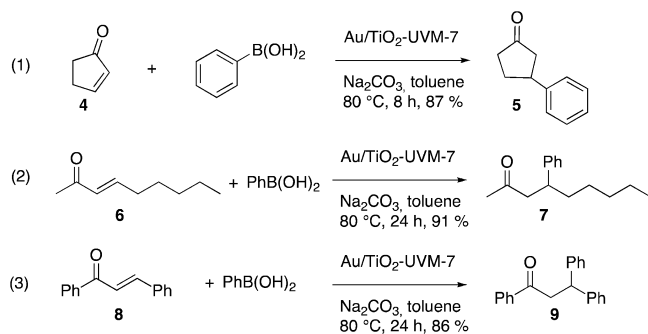
entry	catalyst	additives	ref	3a yield (%)
1	Au/TiO <sub>2</sub> –UVM-7		this work	95 <sup>a</sup>
2	Rh(III)/hydrotalcite	1,5-COD	17a	81 <sup>a</sup>
3	Rh(I)/hydrotalcite		17b	98 <sup>a</sup>
4	Rh(III)/NiZn	1,5-COD	17c	92 <sup>b</sup>
5	RhFAP	1,5-COD	17d	90 <sup>b</sup>

<sup>a</sup>Isolated yield. <sup>b</sup>Calculated yield from GC or <sup>1</sup>H NMR.

compares favorably with other known Rh heterogeneous systems, such as Rh(III)/hydrotalcite, Rh(I)/hydrotalcite, Rh(III)/NiZn, and RhFAP (FAP = fluoroapatite), that require 1,5-COD<sup>17a,c,d</sup> (Table 4, entries 2, 4, 5) as additives or a higher catalytic loading<sup>17b</sup> (Table 4, entry 3).

As preliminary results, the activity of our catalytic system was tested on other enones, such as cyclopenten-2-one **4**, (*E*)-non-3-en-2-one **6**, and (*E*)-1,3-diphenylprop-2-en-1-one **8** (Scheme 3). Under standard conditions, for example, in the presence of

**Scheme 3. 1,4-Addition of Phenylboronic Acid (**2**) to Selected Enones**



1 wt % Au/TiO<sub>2</sub>–UVM-7 at 80 °C in toluene, the reaction of phenylboronic acid with cyclopenten-2-one **4** cleanly allowed the formation of the desired ketone **5** in 87% isolated yield (Scheme 3, eq 1). The reaction conditions were also compatible with an acyclic linear enone, such as (*E*)-non-3-en-2-one **6**, and an aryl-substituted ketone, such as (*E*)-1,3-diphenylprop-2-en-1-one **8**. The enones were transformed to the corresponding 4-phenylnonan-2-one **7** and 1,3,3-triphenylpropan-1-one **9** in excellent isolated yields, 91% and 86%, respectively (Scheme 3, eqs 2, 3).

Mechanistically, we can consider the first step as a transmetalation step based on homogeneous<sup>22</sup> and heterogeneous<sup>5d,e</sup> Au(III) catalysts' activity reports from the literature (Scheme 4). The Lewis acid properties of Au(III) catalyst, as recently highlighted by Toste's group,<sup>23</sup> would favor the 1,4-carbometalation, leading to intermediate **C**. The protodemetalation step followed by dissociation of the arylated ketone would lead to regeneration of the catalyst **A**.

**3.3. Catalyst Stability and Recyclability.** The catalyst stability and recyclability were established by performing three successive reaction tests and characterization of the catalyst

after each reaction. The 1,4-addition of phenylboronic acid (**2a**) to 2-cyclohexen-1-one (**1**) over Au/TiO<sub>2</sub>–UVM-7 was selected as our benchmark reaction. After each step, the catalyst was separated via centrifugation, washed with toluene, and dried at 60 °C for 2 h. As can be seen from Table 5, the recycled

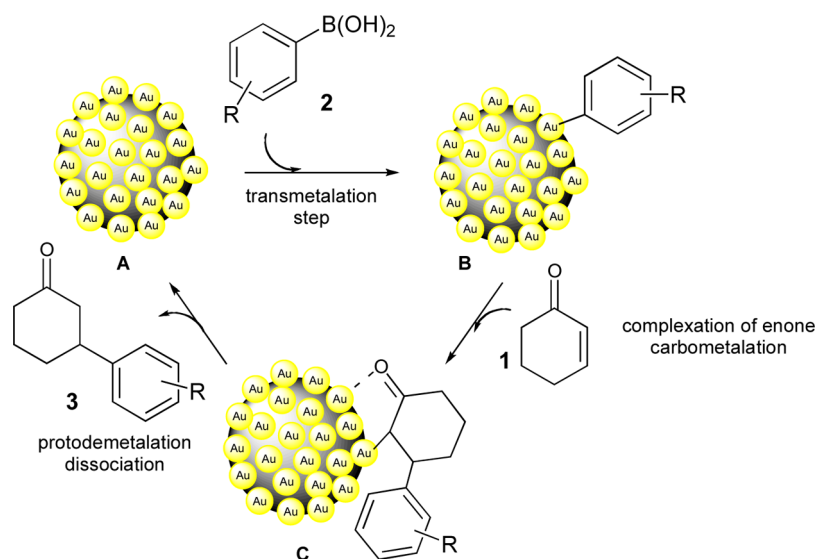
**Table 5. Recycling Tests for 1,4-Addition of Phenylboronic Acid **2a** to 2-Cyclohexen-1-one **1****

run	conversion (%)	isolated yield (%) of <b>3a</b>
1	98	95
2	97	93
3	97	91

supported catalysts did not exhibit any significant loss of activity. Only a slight decrease in the isolated yield was observed after three runs. Moreover, the ICP–OES analysis of the filtered solution after the catalytic tests showed that the gold concentration was below the detection limit of the equipment.

For this reaction, because we worked in toluene medium, the mesostructure resists heating for a long period, which has been corroborated through electron microscopy and N<sub>2</sub> adsorption–desorption isotherms. No significant degradation of the UVM-7-type architecture, according to TEM images, even after three catalytic cycles (Figure 5a), was observed. The architecture based on the aggregation of primary mesoporous nanoparticles was pleasingly preserved. We detected only a slight loss of order in the intraparticle mesopore system; however, this minor structural change may be irrelevant from the catalytic point of view if accessibility to the gold nanoparticles is preserved to a large extent. At this point, the N<sub>2</sub> adsorption–desorption isotherm confirmed that the bimodal hierarchic porosity typical of the UVM-7 support was maintained for the used catalyst. The two adsorption steps and their respective peaks in the BJH pore size distribution could be clearly appreciated in Figure 5c,d, respectively. After being used, only a relatively small decrease in the textural parameters was observed (BET surface area = 547.3 m<sup>2</sup>/g and BJH pore volume = 1.27 cm<sup>3</sup>/g) when compared with the starting catalyst. On the other hand, dealing with the active sites, for example, the gold nanoparticles,

**Scheme 4. Proposed Mechanism for 1,4-Addition of Arylboronic Acid to 2-Cyclohexen-1-one**



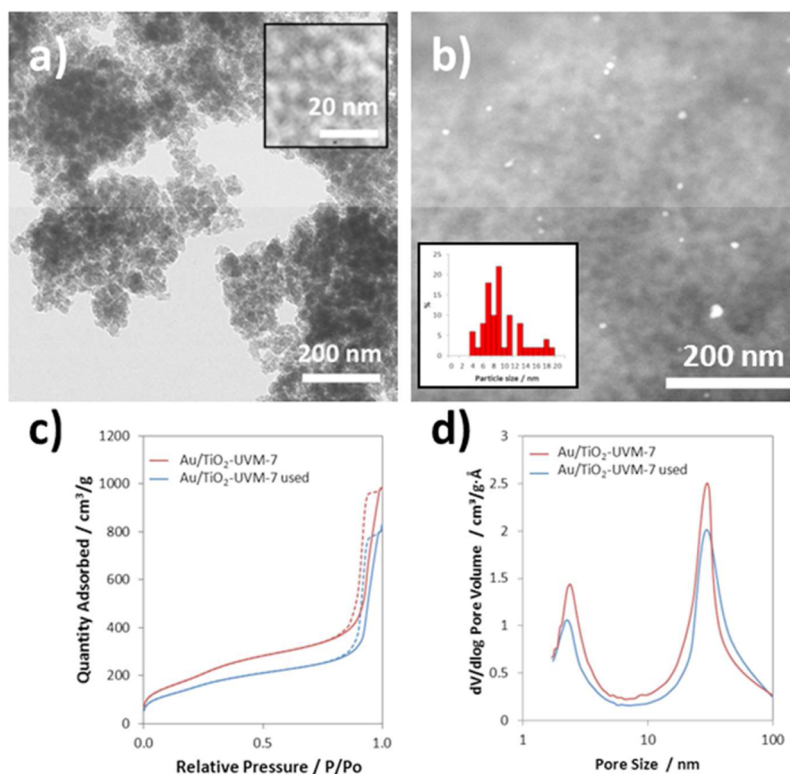


**Figure 5.** (a) TEM, (b) HAADF, and (c)  $N_2$  adsorption–desorption isotherms and (d) BJH pore size distributions of the Au/TiO<sub>2</sub>-UVM-7 material after three catalytic cycles.

although a good dispersion of the gold nanoparticles was preserved according to HAADF (Figure 5b), a small nanoparticle growth (gold particle size from 6.5 to 9.7 nm after three cycles) has been detected. These small changes in the catalyst architecture could explain the low decrease in the catalytic activity during the recycling tests.

## CONCLUSIONS

A silica–titania support was successfully prepared and loaded with 1 wt % gold. The prepared material was shown to be an efficient catalyst in the unprecedented gold-catalyzed 1,4-addition of various functionalized arylboronic acids to 2-cyclohexen-1-one using toluene as a solvent. The reaction conditions were efficiently applied to other selected enones, such as cyclic, linear, and aryl-substituted ones. The addition of phenylboronic acid to 2-cyclohexen-1-one led to a TOF of 18, which is 3–4 times higher than other heterogeneous catalytic systems reported in the literature for this reaction in the presence of rhodium catalysts. The superior activity of the Au/TiO<sub>2</sub>-UVM-7 catalyst was demonstrated compared with other gold-based heterogeneous catalysts and may be explained by the high dispersion of Au, a specific interaction of Au with the dispersed titanium oxide, and the existence of a high accessibility to the active sites, thanks to the hierarchic porosity of UVM-7. The gold-based catalyst was recycled and therefore played an active role in this reaction, the nature of the solvent determining a remarkable change in the products selectivity. Further studies will be dedicated in the study of the generality of this catalytic system toward other Michael acceptors.

## AUTHOR INFORMATION

### Corresponding Authors

\*E-mail: [florentina.neatu@chimie.unibuc.ro](mailto:florentina.neatu@chimie.unibuc.ro).

\*E-mail: [vasile.parvulescu@g.unibuc.ro](mailto:vasile.parvulescu@g.unibuc.ro).

\*E-mail: [pedro.amoros@uv.es](mailto:pedro.amoros@uv.es).

\*E-mail: [veronique.michelet@chimie-paristech.fr](mailto:veronique.michelet@chimie-paristech.fr).

### Notes

The authors declare no competing financial interest.

## ACKNOWLEDGMENTS

This work was supported by a grant from the Romanian Ministry of Education, CNCS–UEFISCDI, Project No. PN-II-RU-PD-2012-3-0295, the Centre National de la Recherche Scientifique (CNRS), the Ministerio de Economía y Competitividad (MAT2012-38429-C04-03), and the Generalitat Valenciana (PROMETEO/2009/108). A.M. thanks MEC for a FPI fellowship.

## REFERENCES

- (1) (a) Haruta, M.; Kobayashi, T.; Sano, H.; Yamada, N. *Chem. Lett.* **1987**, 16, 405–408. (b) Haruta, M. *Catal. Today* **1997**, 36, 153–166. (c) Hughes, M. D.; Xu, Y.-J.; Jenkins, P.; McMorn, P.; Landon, P.; Enache, D. I.; Carley, A. F.; Attard, G. A.; Hutchings, G. J.; King, F.; Stitt, E. H.; Johnston, P.; Griffin, K.; Kiely, C. J. *Nature* **2005**, 437, 1132–1135. (d) Hashmi, A. S. K.; Hutchings, G. J. *Angew. Chem., Int. Ed.* **2006**, 45, 7896–7936. (e) Corma, A.; Serna, P. *Science* **2006**, 313, 332–334. (f) Grierrane, A.; Corma, A.; García, H. *Science* **2008**, 322, 1661–1664. (g) Abad, A.; Corma, A.; García, H. *Chem.—Eur. J.* **2008**, 14, 212–222. (h) Corma, A.; García, H. *Chem. Soc. Rev.* **2008**, 37, 2096–2126. (i) Goguet, A.; Hardacre, C.; Harvey, I.; Narasimharao, K.; Saih, Y.; Sa, J. J. *Am. Chem. Soc.* **2009**, 131, 6973–6975. (j) Aschwanden, L.; Mallat, T.; Maciejewski, M.; Krumeich, F.; Baiker, A. *ChemCatChem* **2010**, 2, 666–673. (k) Zhang, Y.; Cui, X. J.; Shi, F.;



- Deng, Y. Q. *Chem. Rev.* **2012**, *112*, 2467–2505. (l) Boronat, M.; Leyva-Perez, A.; Corma, A. *Acc. Chem. Res.* **2014**, *47*, 834–844. (m) Haruta, M. *Angew. Chem., Int. Ed.* **2014**, *53*, 52–56. (n) Stratakis, M.; Garcia, H. *Chem. Rev.* **2012**, *112*, 4469–4506. (o) Hashmi, A. S. K. *Science* **2012**, *338*, 1434–1434. (p) Oliver-Meseguer, J.; Cabrero-Antonino, J. R.; Domínguez, I.; Leyva-Pérez, A.; Corma, A. *Science* **2012**, *338*, 1452–1455.
- (2) Hakkinen, H. *Chem. Soc. Rev.* **2008**, *37*, 1847–1859.
- (3) (a) Haruta, M.; Tsubota, S.; Kobayashi, T.; Kageyama, H.; Genet, M. J.; Delmon, B. J. *Catal.* **1993**, *144*, 175–192. (b) Lopez, N.; Janssens, T. V. W.; Clausen, B. S.; Xu, Y.; Mavrikakis, M.; Bligaard, T.; Nørskov, J. K. *J. Catal.* **2004**, *223*, 232–235. (c) Chen, M.; Goodman, D. W. *Acc. Chem. Res.* **2006**, *39*, 739–746. (d) Boronat, M.; Corma, A.; Illas, F.; Radilla, J.; Ródenas, T.; Sabater, M. J. *J. Catal.* **2011**, *278*, 50–58.
- (4) (a) Teles, J. H.; Brode, S.; Chabanas, M. *Angew. Chem., Int. Ed.* **1998**, *37*, 1415–1418. (b) Marion, N.; Ramón, R. S.; Nolan, S. P. *J. Am. Chem. Soc.* **2009**, *131*, 448–449. (c) Blanco Jaimes, M. C.; Böhlring, C. R. N.; Serrano-Becerra, J. M.; Hashmi, A. S. K. *Angew. Chem., Int. Ed.* **2013**, *52*, 7963–7966. (d) Blanco Jaimes, M. C.; Rominger, F.; Pereira, M. M.; Carrilho, R. M. B.; Carabineiro, S. A. C.; Hashmi, A. S. K. *Chem. Commun.* **2014**, *50*, 4937–4940. (e) *Modern Gold Catalysis*; Toste, F. D., Hashmi, A. S. K., Eds.; Wiley-VCH: Weinheim, 2012. (f) *Gold Catalysis: An Homogeneous Approach*; Toste, F. D., Michelet, V., Eds.; Imperial College Press: London, 2014.
- (5) (a) Tsunoyama, H.; Sakurai, H.; Ichikuni, N.; Negishi, Y.; Tsukuda, T. *Langmuir* **2004**, *20*, 11293–11296. (b) Sakurai, H.; Tsunoyama, H.; Tsukuda, T. *J. Organomet. Chem.* **2007**, *692*, 368–374. (c) Russell, J. C.; Blunt, M. O.; Garfitt, J. M.; Scurr, D. J.; Alexander, M.; Champness, N. R.; Beton, P. H. *J. Am. Chem. Soc.* **2011**, *133*, 4220–4223. (d) Carrettin, S.; Corma, A.; Iglesias, M.; Sánchez, F. *Appl. Catal., A* **2005**, *291*, 247–252. (e) Carrettin, S.; Guzman, J.; Corma, A. *Angew. Chem., Int. Ed.* **2005**, *44*, 2242–2245. (f) Palashuddin, Sk. Md.; Jana, C. K.; Chattopadhyay, A. *Chem. Commun.* **2013**, *49*, 8235–8237.
- (6) Levin, M. D.; Toste, F. D. *Angew. Chem., Int. Ed.* **2014**, *53*, 6211–6215.
- (7) Han, J.; Liu, Y.; Guo, R. J. *J. Am. Chem. Soc.* **2009**, *131*, 2060–2061.
- (8) (a) Gonzalez-Arellano, C.; Abad, A.; Corma, A.; Garcia, H.; Iglesias, M.; Sanchez, F. *Angew. Chem., Int. Ed.* **2007**, *46*, 1536–1538. (b) de Souza, R. O. M. A.; Bittar, M. S.; Mendes, L. V. P.; da Silva, C. M. F.; da Silva, V. T.; Antunes, O. A. C. *Synlett* **2008**, *2008*, 1777–1780. (c) Kanuru, V. K.; Kyriakou, G.; Beaumont, S. K.; Papageorgiou, A. C.; Watson, D. J.; Lambert, R. M. *J. Am. Chem. Soc.* **2010**, *132*, 8081–8086. (d) Kyriakou, G.; Beaumont, S. K.; Humphrey, S. M.; Antonetti, C.; Lambert, R. M. *ChemCatChem* **2010**, *2*, 1444–1449.
- (9) Karimi, B.; Esfahani, F. K. *Chem. Commun.* **2011**, *47*, 10452–10454.
- (10) Kim, S.; Bae, S. W.; Lee, J. S.; Park, J. *Tetrahedron* **2009**, *65*, 1461–1466.
- (11) Taylor, S. F. R.; Sá, J.; Hardacre, C. *ChemCatChem* **2011**, *3*, 119–121.
- (12) Cheneviere, Y.; Caps, V.; Tuel, A. *Appl. Catal., A* **2010**, *387*, 129–134.
- (13) (a) Ishida, T.; Kawakita, N.; Akita, T.; Haruta, M. *Gold Bull.* **2009**, *42*, 267–274. (b) He, L.; Lou, X.-B.; Ni, J.; Liu, Y.-M.; Cao, Y.; He, H.-Y.; Fan, K.-N. *Chem.—Eur. J.* **2010**, *16*, 13965–13969. (c) Peng, Q.; Zhang, Y.; Shi, F.; Deng, Y. *Chem. Commun.* **2011**, *47*, 6476–6478. (d) Tang, C.-H.; He, L.; Liu, Y.-M.; Cao, Y.; He, H.-Y.; Fan, K.-N. *Chem.—Eur. J.* **2011**, *17*, 7172–7177. (e) Ciobanu, M.; Cojocaru, B.; Teodorescu, C.; Vasiliu, F.; Coman, S. M.; Leitner, W.; Parvulescu, V. I. *J. Catal.* **2012**, *296*, 43–54.
- (14) (a) Carrettin, S.; Blanco, M. C.; Corma, A.; Hashmi, A. S. K. *Adv. Synth. Catal.* **2006**, *348*, 1283–1288. (b) Gryparis, C.; Efe, C.; Raptis, C.; Lykakis, I. N.; Stratakis, M. *Org. Lett.* **2012**, *14*, 2956–2959. (c) Notar Francesco, I.; Giauffret, J.; Fontaine-Vive, F.; Edwards, J. K.; Kiely, C. J.; Hutchings, G. J.; Antonietti, S. *Tetrahedron* **2014**, *70*, 9635–9643. (d) Neatu, F.; Li, Z.; Richards, R.; Toullec, P. Y.; Genet, J.-P.; Dumbuya, K.; Gottfried, J. M.; Steinrueck, H.-P.; Parvulescu, V. I.; Michelet, V. *Chem.—Eur. J.* **2008**, *14*, 9412–9418.
- (15) (a) Corma, A.; Concepción, P.; Domínguez, I.; Forné, V.; Sabater, M. J. *J. Catal.* **2007**, *251*, 39–47. (b) Yamane, Y.; Liu, X.; Hamasaki, A.; Ishida, T.; Haruta, M.; Yokoyama, T.; Tokunaga, M. *Org. Lett.* **2009**, *11*, 5162–5165. (c) So, M.-H.; Liu, Y.; Ho, C.-M.; Lam, K.-Y.; Che, C.-M. *ChemCatChem* **2011**, *3*, 386–393.
- (16) (a) Rittleng, V.; Sirlin, C.; Pfeffer, M. *Chem. Rev.* **2002**, *102*, 1731–1769. (b) He, P.; Lu, Y.; Dong, C.-G.; Hu, Q.-S. *Org. Lett.* **2007**, *9*, 343–346. (c) Horiguchi, H.; Tsurugi, H.; Satoh, T.; Miura, M. *J. Org. Chem.* **2008**, *73*, 1590–1592. (d) Korenaga, T.; Osaki, K.; Maenishi, R.; Sakai, T. *Org. Lett.* **2009**, *11*, 2325–2328. (e) Nishimura, T.; Wang, J.; Nagaosa, M.; Okamoto, K.; Shintani, R.; Kwong, F.-y.; Yu, W.-y.; Chan, A. S. C.; Hayashi, T. *J. Am. Chem. Soc.* **2010**, *132*, 464–465. (f) Luo, Y.; Carnell, A. J. *Angew. Chem., Int. Ed.* **2010**, *49*, 2750–2754. (g) Hansmann, M. M.; Hashmi, A. S. K.; Lautens, M. *Org. Lett.* **2013**, *15*, 3226–3229. (h) Berthon-Gelloz, G.; Hayashi, T. *Boronic Acids Preparation and Applications. In Organic Synthesis, Medicine and Materials*, 2nd ed.; Hall, D. G., Ed.; Wiley-VCH: Weinheim, Germany, 2011; p 263.
- (17) (a) Fujita, N.; Motokura, K.; Mori, K.; Mizugaki, T.; Ebitani, K.; Jitsukawa, K.; Kaneda, K. *Tetrahedron Lett.* **2006**, *47*, 5083–5087. (b) Neatu, F.; Besnea, M.; Komvokis, V. G.; Genet, J. P.; Michelet, V.; Triantafyllidis, K. S.; Parvulescu, V. I. *Catal. Today* **2008**, *139*, 161–167. (c) Hara, T.; Fujita, N.; Ichikuni, N.; Wilson, K.; Lee, A. F.; Shimazu, S. *ACS Catal.* **2014**, *4*, 4040–4046. (d) Noda, H.; Motokura, K.; Chun, W.-J.; Miyaji, A.; Yamaguchi, S.; Baba, T. *Catal. Sci. Technol.* **2015**, *5*, 2714–2727. (e) Kantam, M. L.; Subrahmanyam, V. B.; Shiva Kumar, K. B.; Venkanna, G. T.; Sreedhar, B. *Helv. Chim. Acta* **2008**, *91*, 1947–1953. (f) Handa, P.; Holmberg, K.; Sauthier, M.; Castanet, Y.; Mortreux, A. *Microporous Mesoporous Mater.* **2008**, *116*, 424–431.
- (18) (a) El Haskouri, J.; Ortiz de Zarate, D.; Guillem, C.; Latorre, J.; Caldes, M.; Beltran, A.; Beltran, D.; Descalzo, A. B.; Rodriguez-Lopez, G.; Martinez-Manez, R.; Marcos, M. D.; Amoros, P. *Chem. Commun.* **2002**, *38*, 330–331. (b) El Haskouri, J.; Morales, J. M.; Ortiz de Zarate, D.; Fernandez, L.; Latorre, J.; Guillem, C.; Beltran, A.; Beltran, D.; Amoros, P. *Inorg. Chem.* **2008**, *47*, 8267–8277. (c) Perez-Cabero, M.; Hungria, A. B.; Morales, J. M.; Tortajada, M.; Ramon, D.; Moragues, A.; El Haskouri, J.; Beltran, A.; Beltran, D.; Amoros, P. *J. Nanopart. Res.* **2012**, *14*, 12.
- (19) Ortlam, A.; Rathousky, J.; SchulzEkloff, G.; Zukal, A. *Microporous Mater.* **1996**, *6*, 171–180.
- (20) (a) Neatu, F.; Parvulescu, V. I.; Michelet, V.; Genet, J.-P.; Goguet, A.; Hardacre, C. *New J. Chem.* **2009**, *33*, 102–106. (b) Neatu, F.; Toullec, P. Y.; Michelet, V.; Parvulescu, V. I. *Pure Appl. Chem.* **2009**, *81*, 2387–2396. (c) Opris, C. M.; Pavel, O. D.; Moragues, A.; El Haskouri, J.; Beltran, D.; Amoros, P.; Marcos, M. D.; Stoflea, L. E.; Parvulescu, V. I. *Catal. Sci. Technol.* **2014**, *4*, 4340–4355.
- (21) Puértolas, B.; Mayoral, Á.; Arenal, R.; Solsona, B.; Moragues, A.; Murcia-Mascaros, S.; Amorós, P.; Hungria, A. B.; Taylor, S. H.; García, T. *ACS Catal.* **2015**, *5*, 1078–1086.
- (22) (a) Brenzovich, W. E.; Benitez, D.; Lackner, A. D.; Shunatona, H. P.; Tkatchouk, E.; Goddard, W. A., III; Toste, F. D. *Angew. Chem., Int. Ed.* **2010**, *49*, 5519–5522. (b) Tkatchouk, E.; Mankad, N. P.; Benitez, D.; Goddard, W. A., III; Toste, F. D. *J. Am. Chem. Soc.* **2011**, *133*, 14293–14300. (c) Zhang, G.; Cui, L.; Wang, Y.; Zhang, L. *J. Am. Chem. Soc.* **2010**, *132*, 1474–1475.
- (23) (a) Wu, C.-Y.; Horibe, T.; Jacobsen, C. B.; Toste, F. D. *Nature* **2015**, *517*, 449–454. (b) For a recent highlight, see: Teles, J. H. *Angew. Chem., Int. Ed.* **2015**, *54*, 5556–5558 and references cited therein.